Catalysis Today 180 (2012) 19–24

Contents lists available at ScienceDirect

Catalysis Today

journal homepage: www.elsevier.com/locate/cattod

Water gas shift reaction on carbon-supported Pt catalysts promoted by CeO_2

R. Buitrago, J. Ruiz-Martínez, J. Silvestre-Albero, A. Sepúlveda-Escribano*, F. Rodríguez-Reinoso

Laboratorio de Materiales Avanzados, Instituto Universitario de Materiales de Alicante, Departamento de Química Inorgánica, Universidad de Alicante, Apartado 99, E-03080 Alicante, Spain

ARTICLE INFO

Article history:
Received 1 February 2011
Received in revised form 23 June 2011
Accepted 9 July 2011
Available online 25 August 2011

Keywords:
Carbon support
CeO_2
Platinum
WGS

ABSTRACT

The low temperature water gas shift reaction has been studied over carbon-supported platinum catalysts promoted by ceria. To this end, CeO_2 has been dispersed over an activated carbon support at different loadings (20, 30 and 40 wt.%) in order to obtain a high ceria surface area. Then, platinum has been incorporated by impregnation with an acetone solution of $[Pt(NH_3)_4](NO_3)_2$. Two more catalysts have been prepared with aqueous and ethanolic solutions, respectively, to assess the effect of the solvent in the final catalysts. Pt/CeO_2 and Pt/C catalysts have been used as references. Catalysts have been characterized (N_2 adsorption at 77 K, TEM, H_2-TPR) and tested in reaction after reduction with H_2 at 473 K. The obtained results show that CO conversion increases with the amount of ceria loaded, from 20 to 40 wt.%. At this temperature, platinum supported on bulk CeO_2 is less active than its carbon-based counterparts. The best results are obtained for the catalysts with 40 wt.% CeO_2 prepared by aqueous impregnation of the platinum precursor, which achieves conversions higher than 70% at 573 K, and shows no deactivation under reaction at this temperature for 120 h. On the other hand, Pt/C shows a very low activity, this certifying the determinant role of ceria in this reaction. These results indicate that dispersion of ceria on activated carbon allows to obtain catalysts with superior performance than using bulk CeO_2 as support, and with a lesser amount of ceria.

1. Introduction

Nowadays, the depletion of fossil fuels and the environmental problems associated to their use as energy sources encourage the research towards other energy models, both renewable and sustainable. In this scenario, hydrogen arises as an energy vector that can fulfil these requirements [1–3]. However, although hydrogen is the most abundant element on the Earth, it cannot be found as a single element, and it is necessary to synthesize it from hydrogen-containing compounds. In conventional plants, hydrogen is produced by the steam reforming of methane and other hydrocarbons. However, this process also produces CO. The presence of CO can be useful if steam reforming is addressed to the production of synthesis gas ($CO + H_2$, in different ratios), but it is highly undesirable if hydrogen is going to be used in applications such as electricity generation by polymer electrolyte fuel cells (PEM) [4,5], where CO is a severe poison for platinum catalysts in the electrodes.

The water–gas shift reaction has been used for long time, coupled with the steam reforming of hydrocarbons, to modulate the CO/H_2 ratio of the produced gas stream or even for nearly completely removing poisonous CO, as in the case of ammonia synthesis:

$$CO_{(g)} + H_2O_{(g)} \leftrightarrow CO_{2(g)} + H_{2(g)} \qquad \Delta H_{298\,K^\circ} = -41.2\ \text{kJ/mol}$$

Because of its exothermic character and the existence of thermodynamic limitations at high temperatures, this reaction has been carried out through two stages: the high-temperature shift (623–643 K) with iron-based catalysts [6], and the low-temperature shift (473–493 K) with copper-based catalysts [7]. In this sense, it is highly desirable to develop an active catalyst that could work at temperatures as low as possible. Although the commercial Cu–ZnO based catalysts are extensively used, they show important disadvantages: they need long-term activation procedures, they are pyrophoric, and they are intolerant to poisons, condensation and oxidation [8].

Several catalysts, including different metals and supports, have been investigated for the low-temperature water gas shift reaction for fuel cell applications. Among them, CeO_2 supported platinum arises as the one of the most promising [9–11]. Ceria is a partially reducible oxide whose surface reducibility is strongly enhanced in the presence of a noble metal, which not only lowers the reduction temperature but also increases the extent of reduction. One of the proposed mechanisms for WGS involves the chemisorption of CO on the metal particles and its subsequent oxidation by the support, through the interaction with active OH groups on the ceria surface,

---

* Corresponding author. Tel.: +34 965 90 3974; fax: +34 965 90 3454.
E-mail address: asepul@ua.es (A. Sepúlveda-Escribano).

0920-5861/$ – see front matter © 2011 Elsevier B.V. All rights reserved.
doi:10.1016/j.cattod.2011.07.032

yielding surface formates. Then, water decomposes the surface formates to give hydrogen and CO_2, this re-oxidising the ceria surface [12,13]. In this sense, it seems clear that the role of the ceria surface is determinant for this reaction, both in terms of extension (large surface areas are needed) but also in terms of reducibility. On the other hand, the limited supply and extensive applications of this oxide make it also necessary to optimize its use. With this background, the aim of this work has been to prepare optimized CeO_2-promoted Pt catalysts in which the interaction between the metal and the oxide is enhanced, and a large ceria surface is available while reducing the ceria amount in the catalyst. To this end, CeO_2 has been dispersed on a high surface area activated carbon. It has been previously shown in other works from our group that large ceria dispersions (low ceria crystallite sizes) can be achieved by this approach, and that this approach can be used to enhance the catalytic behavior in different reactions [14–17].

2. Experimental

2.1. Catalyst preparation

The support was an industrial activated carbon (IZASA) prepared from olive stones by direct steam activation, and labeled as C. It was washed with diluted H_2SO_4 to remove the main part of its inorganic material, and then with distilled water until no sulfates were detected. After drying, the carbon was grinded and meshed (200–300 μm), and stored in the oven at 373 K overnight. For the cerium precursor impregnation, the corresponding amount of $Ce(NO_3)_3{\cdot}6H_2O$ (99.99%, Sigma–Aldrich) was dissolved in acetone. Dried carbon was added to the solution, in a proportion of 10 mL/g of support, with stirring. After 12 h in a covered flask, the excess of solvent was slowly removed by flowing nitrogen at room temperature, and the sample was finally dried under vacuum until complete removal of the solvent. Finally, the solid was heat treated during 5 h at 623 K under flowing helium (50 mL/min), with a heating rate of 1 K min^{-1}, in order to slowly decompose the cerium nitrate to form CeO_2, trying to avoid the modification of the carbon surface by the evolved nitrogen oxides [14]. Three CeO_2/C samples were prepared in this way with different CeO_2 loadings: 20, 30 and 40 wt.%.

Platinum addition on CeO_2/C was carried out using the proper amount of $[Pt(NH_3)_4](NO_3)_2$ (99.9%, Sigma–Aldrich) dissolved in acetone to obtain 1 wt.% Pt, with 10 mL of solution per gram of solid. After stirring for 12 h, the solvent was removed under vacuum at 333 K. Finally, the catalysts were treated at 673 K for 5 h under flowing He (50 mL/min). In this way, three catalysts were prepared which are labeled as Pt–20Ce/C, Pt–30Ce/C and Pt–40Ce/C. Two more catalysts, Pt–40Ce/C Aq and Pt–40Ce/C Et, have been prepared in the same way but using water and ethanol, respectively, as solvents for the platinum precursor. For the sake of comparison, a Pt/CeO_2 catalyst was also synthesized. CeO_2 was prepared by precipitation from an aqueous solution of $Ce(NO_3)_3{\cdot}6H_2O$ (99.99%, Sigma–Aldrich) containing an excess of urea. The solution was heated at 363 K and kept at this temperature, with slow stirring, for 12 h. The solid formed was filtered and calcined at 673 K for 4 h. The CeO_2 support prepared in this way was impregnated with the Pt precursor as described for the carbon supported catalysts. Finally, a Pt/C catalyst was also prepared, following the same impregnation method, in order to check the effect of the carbon support in the reaction. After preparation, the catalyst was heat treated under N_2 flow (50 mL/min) at 673 K for 4 h.

2.2. Catalyst characterization

The actual ceria content of Ce/C supports was determined by burning off the carbon in air at 973 K and weighting the residue, using the parent activated carbon as a blank. With regard to Pt, the amount loaded was determined by burning off the carbon support and analyzing the residue (dissolved in Aqua Regia) by UV spectrophotometry (wavelength = 261.8 nm). The determined loadings, both of ceria and platinum, fitted the nominal ones within the experimental error.

Textural properties of the prepared materials were determined by nitrogen adsorption at 77 K on a Coulter Omnisorp 610 system. Before measurements, the samples were dried at 383 K for 12 h and out-gassed at 523 K under vacuum. The micropore volume, V_{micro}, was obtained by application of the Dubinin–Radushkevich (DR) equation to the adsorption isotherm. The volume of mesopores, V_{meso}, was estimated by subtracting the micropore volume from the uptake at a relative pressure of 0.95. The surface area was calculated by application of the B.E.T. method.

X-ray powder diffraction patterns were recorded on a JSO Debye-flex 2002 system, from Seifert, fitted with a Cu cathode and a Ni filter, using a 2° min^{-1} scanning rate.

Temperature-programmed reduction (TPR) measurements were carried out in a U-shaped quartz cell using a 5% H_2/He gas flow of 25 $cm^3\ min^{-1}$ and about 0.15 g of sample, with a heating rate of 10 K min^{-1}. Hydrogen consumption was followed by on-line mass spectrometry.

Conventional TEM analysis was carried out with a JOEL model JEM-210 electron microscope working at 200 kV and equipped with a INCA Energy TEM 100 analytical system and a SIS MegaView II camera. Samples for analysis were suspended in methanol and placed on copper grids with a holey-carbon film support.

2.3. Catalytic activity measurements

The catalytic behavior of the prepared samples in the low temperature water–gas shift reaction was evaluated in a fixed bed flow reactor under atmospheric pressure in a range of temperatures from 473 K to 623 K. The feed gas stream prepared contained a volume composition of 1.75% CO, 34.45% H_2, 35.92% H_2O, and He balance, with a total flow of 100 mL/min. Activity tests were performed using 0.100 g of catalyst diluted with SiC, at a volume ratio of 1:2, to avoid thermal effects. Prior to reaction, the catalysts were reduced during 1 h at 673 K. The composition of the gas stream exiting the reactor was determined by mass spectrometry (Pfeiffer, OmniStar GSD 301), and the catalytic activity will be expressed by degree of CO conversion. Reaction at each temperature was stabilized for 1 h.

3. Results and discussion

3.1. Textural characterization

Table 1 shows the specific surface area (N_2, 77 K, BET), the micropore volume (V_{micro}, N_2, 77 K, D-R) and the volume of mesopores (V_{meso}) for the parent carbon, the three ceria-loaded carbons, the three platinum catalysts prepared with the ceria-loaded carbons as support and the Pt/Ce catalyst which uses massive CeO_2 as sup-

Table 1
Textural properties of supports and catalyst.

	S_{BET} (m^2/g)	V_{micro} ($cm^3\ g^{-1}$)	V_{meso} ($cm^3\ g^{-1}$)
C	1487	0.54	0.62
20Ce/C	1194	0.43	0.52
30Ce/C	1089	0.39	0.43
40Ce/C	982	0.35	0.39
Pt–20Ce/C	1163	0.42	0.43
Pt–30Ce/C	1078	0.39	0.42
Pt–40Ce/C	1009	0.36	0.41
Pt/Ce	45	0.02	–

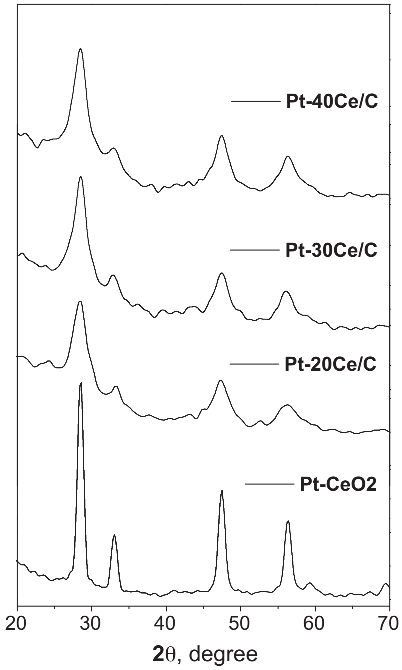

	D(nm)
CeO_2	12.7
20Ce/C	4.4
30Ce/C	6.6
Ce40/C	6.5
Pt20Ce/C	5.5
Pt30Ce/C	5.2
Pt40Ce/C	5.4

Fig. 1. Powder X-ray diffraction patterns of Pt–Ce/C and Pt/Ce catalysts.

port. The N_2 adsorption isotherms at 77 K for all the carbon-based materials (not shown) correspond to type I isotherms, which is characteristic of microporous materials. However, there is also a given amount of mesoporosity, as the adsorption and desorption branches are not coincident (hysteresis loop) above a relative pressure of 0.5. In fact, the mesoporous volume is always slightly larger than the microporous volume.

There is a continuous decrease in the BET surface area for the ceria-loaded carbons as the amount of ceria increases, and the same trend is obtained for both the microporous and the mesoporous volumes. This effect has been previously reported [14] and it is attributed to the blockage of porosity by ceria crystallites to a certain extent. It has also to be taken into consideration that the presence of ceria would lower the textural parameters of these materials as compared with those of the parent carbon, as an effect of the increase of mass and of the much lower porosity of ceria as compared with the carbon. In any case, the fact that both the micro- and mesoporous volumes decrease in the same way is indicative of a good dispersion of ceria through the carbon surface.

The impregnation stage with the platinum precursor, followed by the thermal treatment under helium, has very little effect on the surface parameters of the support. It can be then concluded that platinum is deposited without modifying the previously deposited CeO_2.

Finally, it has to be noted the much lower surface area of the ceria supported platinum catalyst as compared to that of the carbon-based counterparts.

3.2. X-ray diffraction

Fig. 1 shows the XRD patterns of all catalyst prepared, where the characteristic CeO_2 peaks (JCPDS 34-0394) at 28.6, 33.4, 47.8 and 56.7°, corresponding to the reflections in the (1 1 1), (2 0 0), (2 2 0) and (3 3 1) crystalline planes of the cubic fluorite type phase, can be clearly observed. By application of the Scherrer equation to the (1 1 1) diffraction peak, the mean crystal sizes of CeO_2 in the different catalysts have been determined, and they are presented in the table inserted in Fig. 1. Whereas the XRD profile of Pt/Ce shows very narrow diffraction peaks, this indicating a high crystallinity and large crystal size, the diffraction peaks obtained with the carbon supported catalysts are much wider. This is consistent with a smaller crystal size and a high dispersion of CeO_2. Thus, a large exposed surface is expected in these materials, in spite of the fact that they contain a lower amount of CeO_2 than Pt/Ce. On the other hand, no diffraction peaks due to platinum crystallites could be detected, this indicating a good dispersion of the metal phase.

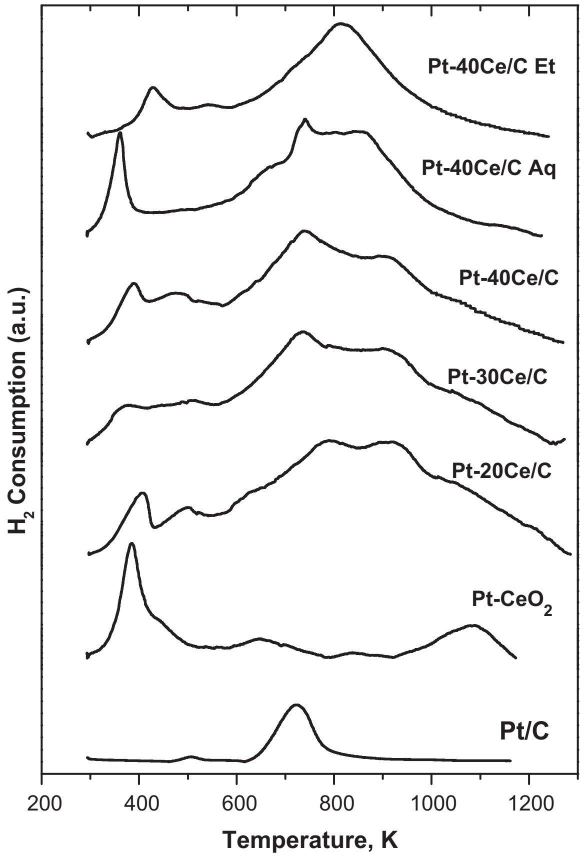

Fig. 2. H_2-TPR profiles for samples under study.

3.3. Temperature programmed reduction

Fig. 2 shows the evolution of H_2 consumption as a function of temperature for the platinum catalysts prepared. The TPR profile obtained with Pt/CeO_2 is similar to others found in the literature [18–21]. The first intense peak centered at about 373 K is assigned to the surface reduction of ceria in close contact with the metal, as well as the platinum reduction (breakdown of Pt–O–CeO_2 species formed upon calcination). There are three more hydrogen consumption peaks (a shoulder of the low temperature peak at 423 K and two more peaks at 653 and at 833 K), which are assigned to the surface reduction of CeO_2 with less and less interaction with the platinum particles. It has to be taken into account that surface ceria reduction in this system takes place by a mechanism by which hydrogen molecules are first adsorbed and dissociated on the platinum particles and, then, spilt over the support, which is reduced by atomic hydrogen. Finally, the broad peak at 1073 K corresponds to the bulk reduction of CeO_2.

Dispersion of CeO_2 on the carbon support produces, as commented above, smaller ceria particles with a larger contribution of surface ceria. This is clearly seen in the TPR profiles of the Pt–Ce/C catalysts, where up to five reduction peaks can be observed.

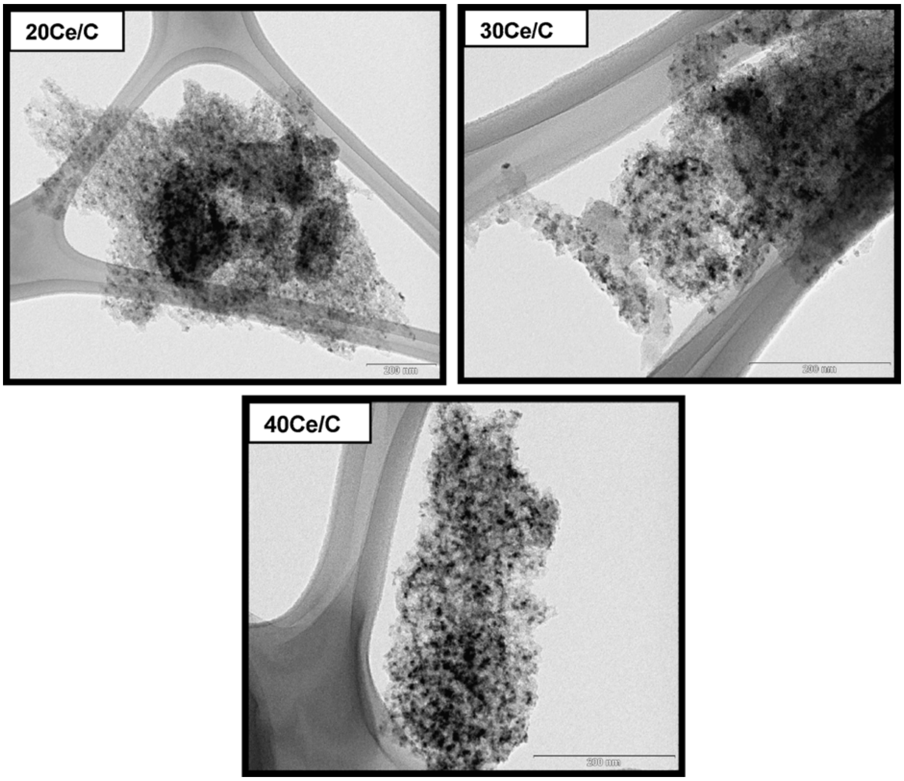

Fig. 3. TEM micrographs of the Ce/C supports (scale bar 200 nm).

The peak assignation is similar to that for the Pt/Ce catalysts: the first low temperature peak corresponds to reduction of platinum species together with ceria in intimate contact with platinum, the higher temperature one (at about 1073 K, now being overlapped with the others) corresponds to bulk reduction of ceria, and the intermediate ones correspond to the surface reduction of ceria which interacts with the platinum particle to different extents. The total hydrogen consumption increases with the amount of ceria loaded on the carbon support, and it is much higher than that for the Pt/Ce catalysts. Thus, reducibility of ceria has increased due to the presence of small particles on the activated carbon support.

It is important to note here the distinctive TPR profile of catalyst Pt–40Ce/C Aq, which shows an intense low temperature reduction peak similar to that obtained with Pt/CeO$_2$. This result indicates that platinum particles in this catalyst are mainly in close contact with ceria crystallites. In this kind of systems, where ceria is dispersed on the carbon support, platinum particles introduced in a subsequent step can be located on the carbon support and/or on the ceria promoter, the former being inactive for the WGS reaction. Thus, to take advantage of the small crystal size of ceria obtained by its dispersion on the carbon support, it is necessary to achieve platinum deposition very close or onto the oxide particles and, in this way, an improved interaction between metal an promoter which results in an improved catalytic behavior.

3.4. *Transmission electron microscopy*

Fig. 3 shows the TEM micrographs of the cerium-based supports. It can be seen that the cerium oxide particles are well dispersed on the carbon support, and no agglomerations are observed. Similar micrographs are obtained for the Pt–Ce/C catalysts (not shown), this confirming that the addition of Pt does not produce important morphological changes in the catalyst.

3.5. *Catalytic activity*

Fig. 4 displays the catalytic activity results of the different samples, in terms of CO conversion as a function of temperature. Activity at each temperature has been determined after 1 h stabilization, and no deactivation was detected during this period.

It can be seen that the Pt/C catalyst is inactive for this reaction, this reflecting the essential role of ceria in this reaction. Furthermore, the catalytic activity of the Ce/C supports were also checked, and conversions lower than 5% were obtained in all cases.

For the carbon-supported catalysts prepared with acetone as solvent for the platinum precursor, there is a clear effect of the ceria loading on the catalytic activity, catalyst Pt–40Ce/C being the most active one. Only at the highest temperature tested, 623 K, the three

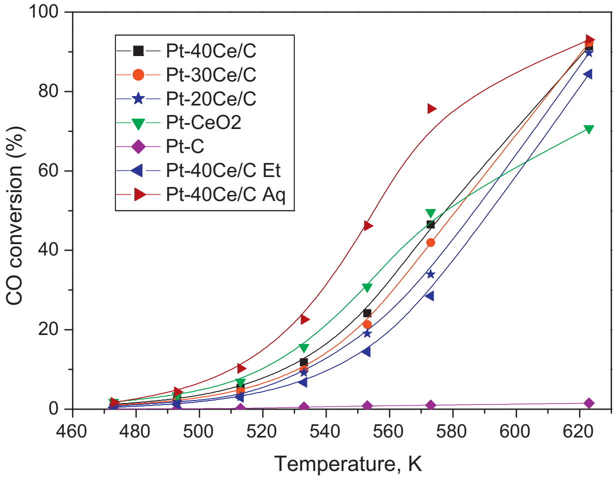

Fig. 4. CO conversion vs. reaction temperature.

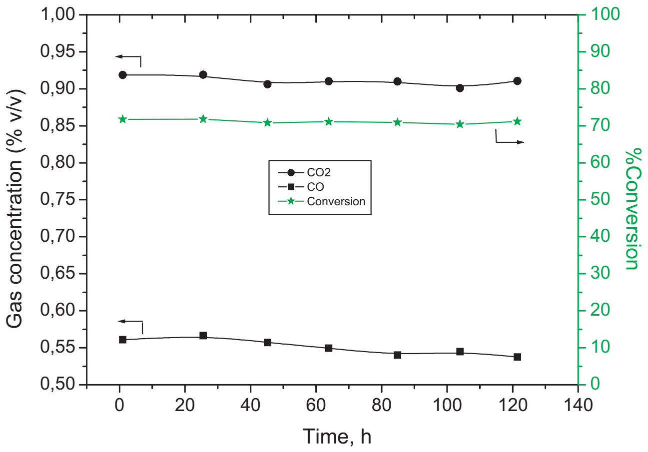

Fig. 5. Stability test for catalyst Pt–40C/Ce Aq. Reaction at 573 K.

catalysts show the same activity close to 90%. It can be seen that Pt/CeO_2 is more active than the latest ones at temperatures below 573 K, but there is an inflexion point at about this temperature in such a way that, from then on, activity increases more slowly with temperature.

The effect of the solvent used during the impregnation of the platinum precursor is clearly manifested by the distinctive behavior of catalysts Pt–40Ce/C (acetone), Pt–40Ce/C Et (ethanol) and Pt–40Ce/C Aq (water). The best catalytic behavior among all the samples prepared has been obtained with catalyst Pt–40Ce/C Aq, which is even better than the model Pt/CeO_2.

During the latest years there have been a lot of studies on the catalytic behavior of Pt/CeO_2 catalyst for the water gas shift reaction [22–25], and the synergism between the noble metal and the oxide support is clearly established [13,26]. There are two proposed mechanisms for this reaction, the interaction between the noble metal and the oxide support being of pristine importance for both of them: the redox mechanism and the associative mechanism. In the redox mechanism, CO adsorbed on the metal surface would reduce the oxide at the metal–oxide interface yielding CO_2, whereas H_2O would reoxidize the support to yield H_2. In the associative mechanism [12], water is first activated at the vacancies of the oxide surface to generate surface hydroxyl groups; then CO is proposed to react with these hydroxyl groups to form surface formates, which would dehydrogenate on the metal particles to yield H_2 and CO_2. Thus, independently of the mechanism, it is convenient to use high surface area ceria as support to obtain active catalysts [23,27]. The approach used in this work to obtain high surface area ceria has been to prepare it well dispersed on a high surface area activated carbon. Furthermore, a lesser amount of ceria is needed as compared with when it is used as a massive support, and this is very important taking into account the limited supply of this rare earth oxide and its high applicability. TEM micrographs (Fig. 3) have shown that even with the larger ceria loading used, the carbon surface is not completely covered by ceria. That implies that the platinum particles may be located both on the ceria patches and on the bare carbon surface, their catalytic behavior being completely different. This heterogeneity is clearly evidenced by the complex TPR profile, suggesting different degrees of Pt–CeO_2 interaction, and can explain the increase in catalytic activity with increasing the amount of ceria loaded, this increasing the available ceria surface area and also the interaction between the oxide and the noble metal. It has also been shown that the preparation method can help to obtain catalysts with improved platinum–ceria interaction, as it has been the case with the choice of water as solvent for the platinum precursor, instead of acetone or ethanol. The relationship between metal–ceria interaction (as deduced from H_2-TPR) and catalytic behavior has been clearly established.

It is also worthy of commenting that the Pt/CeO_2 catalyst is much less active than the carbon-based counterparts at higher temperatures (data at 673 K) where the Pt–Ce/C catalysts achieve 80–90% CO conversion. Experimental work is being conducting to try to understand the reasons of this behavior.

Finally, a stability test has been carried out on the most active catalyst, Pt–40Ce/C Aq, at 573 K. Fig. 5 shows the evolution of CO conversion and CO/CO_2 concentrations in the gas stream as a function of time. It can be seen that no deactivation is produced up to 120 h on stream.

4. Conclusions

The water gas shift reaction over platinum supported on ceria-loaded activated carbon catalysts (Pt–Ce/C) has been studied. Cerium oxide has been dispersed on the activated carbon surface in order to obtain small ceria particles and a highly available surface area. Platinum has then been introduced by using $[Pt(NH_3)_4][NO_3]_2$ as precursor. It has been shown that the CO conversion increases with the amount of ceria loaded, from 20 to 40 wt.%, achieving around 90% CO conversion at 623 K. It is interesting to highlight that the Pt/Ce catalyst, using massive CeO_2 as support, is slightly more active than the carbon-based catalysts only at low temperatures, below 573 K, whereas at 623 K it achieves a CO conversion of only 70% vs. 90% conversion achieved by its counterparts. The use of water as solvent for the platinum precursor during the impregnation step allow to obtain a catalyst with enhanced platinum–ceria interaction (H_2-TPR), which is attributed to the platinum particles being located very close or onto the ceria particles. This high interaction results in a catalyst with enhanced catalytic behavior as compared with its counterparts, with 75% conversion at 573 K which is stable at least up to 120 h on stream.

The results obtained in this study permit to conclude that this kind of catalysts are promising for the water–gas shift reaction, allowing to decrease the amount of ceria needed to obtain high CO conversions by increasing its available surface area.

Acknowledgements

Financial support from MEC (MAT2007-61734 FEDER) and Generalitat Valenciana (PROMETEO/2009/002 FEDER) is gratefully acknowledged. J.S.A. acknowledges support from MEC, GV and UA (RyC2137/06). R.B. acknowledges the UA, CAM and Union Fenosa for his grant (UF2007-X9159987F).

References

[1] www.hydrogen.energy.gov.
[2] Hydrogen energy and fuel cells, EUR 20719 EN, Special report.
[3] www.eia.doe.gov.
[4] C.G. Farrell, C.L. Gardner, M. Ternan, J. Power Sources 171 (2007) 282–293.
[5] X. Cheng, Z. Shi, N. Glass, L. Zhang, J. Zhang, D. Song, Z. Liu, H. Wang, J. Shen, J. Power Sources 165 (2007) 739–756.
[6] D.S. Newsome, Catal. Rev. Sci. Eng. 21 (1980) 275–318.
[7] F. Huber, H. Meland, M. Roning, H. Venvik, A. Holmen, Top. Catal. 45 (2007) 101–104.
[8] J.M. Zale, D.G. Löffler, J. Power Sources 111 (2002) 58–64.
[9] P. Panagiotopoulou, J. Papavasiliou, G. Avgouropoulos, T. Ioannides, D.I. Kondarides, Chem. Eng. J. 134 (2007) 16–22.
[10] C.M.Y. Yeung, S.C. Tsang, J. Mol. Catal. A: Chem. 322 (2010) 17–25.
[11] G. Jacobs, B.H. Davis, Appl. Catal. A: Gen. 333 (2007) 192–201.
[12] T. Shido, Y. Iwasawa, J. Catal. 141 (1993) 71–81.
[13] G. Jacobs, E. Chenu, P.M. Patterson, L. Williams, D. Sparks, G. Thomas, B.H. Davis, Appl. Catal. A: Gen. 258 (2004) 203–214.
[14] J.C. Serrano-Ruiz, E.V. Ramos-Fernández, J. Silvestre-Albero, A. Sepúlveda-Escribano, F. Rodríguez-Reinoso, Mater. Res. Bull. 43 (2008) 1850–1857.
[15] E.V. Ramos-Fernández, J.C. Serrano-Ruiz, J. Silvestre-Albero, A. Sepúlveda-Escribano, F. Rodríguez-Reinoso, J. Mater. Sci. 43 (2008) 1525–1531.

[16] J.C. Serrano-Ruiz, A. Sepúlveda-Escribano, F. Rodríguez-Reinoso, D. Duprez, J. Mol. Catal. A: Chem. 268 (2007) 227–234.
[17] J.C. Serrano-Ruiz, A. Sepúlveda-Escribano, F. Rodríguez-Reinoso, J. Catal. 246 (2007) 158–165.
[18] A. Sepúlveda-Escribano, F. Coloma, F. Rodríguez-Reinoso, J. Catal. 178 (1998) 649–657.
[19] G. Jacobs, R.A. Keogh, B.H. Davis, J. Catal. 245 (2007) 326–337.
[20] C. Leitenburg, A. Trovarelli, J. Kaspar, J. Catal. 166 (1997) 98–107.
[21] J.C. Serrano-Ruiz, J. Luettich, A. Sepúlveda-Escribano, F. Rodríguez-Reinoso, J. Catal. 241 (2006) 45–55.
[22] Y.-T. Kim, E.-D. Park, H.-C. Lee, D. Lee, K.-H. Lee, Appl. Catal. B: Environ. 90 (2009) 45–54.
[23] T. Bunluesin, R.J. Gorte, G.W. Graham, Appl. Catal. B: Environ. 15 (1998) 107–114.
[24] G. Jacobs, U.M. Graham, E. Chenu, P.M. Patterson, A. Dozier, B.H. Davis, J. Catal. 229 (2005) 499–512.
[25] D. Pierre, W.J. Deng, M. Flytzani-Stephanopoulos, Top. Catal. 107–108 (2005) 920–925.
[26] Y. Li, Q. Fu, M. Fytzani-Stephanopoulos, Appl. Catal. B: Environ. 27 (2000) 179–191.
[27] Q. Fu, H. Saltsburg, M. Flytzani-Stephanopoulos, Science 301 (2003) 935–938.